

MARTIN MARIETTA ENERGY SYSTEMS LIBRARIES



3 4456 0283940 9

ORNL/TM-10896

**ornl**

**OAK RIDGE  
NATIONAL  
LABORATORY**

**MARTIN MARIETTA**

**Corrosion of  
Materials in Chemical Heat  
Pump Working Fluids**

J. H. DeVan  
J. S. Wolf

OAK RIDGE NATIONAL LABORATORY

CENTRAL RESEARCH LIBRARY

CIRCULATION SECTION

SYSTEM GUIDE 123

**LIBRARY LOAN COPY**

DO NOT TRANSFER TO ANOTHER PERSON

If you wish someone else to see this report, send us name with report and the library will arrange a loan.

U.S. GOVERNMENT PRINTING OFFICE: 1975

OPERATED BY  
MARTIN MARIETTA ENERGY SYSTEMS, INC.  
FOR THE UNITED STATES  
DEPARTMENT OF ENERGY

Printed in the United States of America. Available from  
National Technical Information Service  
U.S. Department of Commerce  
5285 Port Royal Road, Springfield, Virginia 22161  
NTIS price codes—Printed Copy: A-04Microfiche: A01

This report was prepared as an account of work sponsored by an agency of the United States Government. Neither the United States Government nor any agency thereof, nor any of their employees, makes any warranty, express or implied, or assumes any legal liability or responsibility for the accuracy, completeness, or usefulness of any information, apparatus, product, or process disclosed, or represents that its use would not infringe privately owned rights. Reference herein to any specific commercial product, process, or service by trade name, trademark, manufacturer, or otherwise, does not necessarily constitute or imply its endorsement, recommendation, or favoring by the United States Government or any agency thereof. The views and opinions of authors expressed herein do not necessarily state or reflect those of the United States Government or any agency thereof.

Metals and Ceramics Division

CORROSION OF MATERIALS IN CHEMICAL HEAT PUMP WORKING FLUIDS

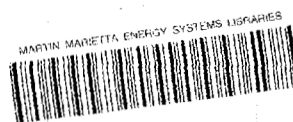
J. H. DeVan and J. S. Wolf

Date Published - November 1988

Prepared for the  
Assistant Secretary for Conservation and Renewable Energy,  
Office of Industrial Programs, Waste Energy  
Recovery Program  
ED 01 01 00 0

NOTICE: This document contains information of a preliminary nature. It is subject to revision or correction and therefore does not represent a final report

Prepared by the  
OAK RIDGE NATIONAL LABORATORY  
Oak Ridge, Tennessee 37831  
operated by  
MARTIN MARIETTA ENERGY SYSTEMS, INC.  
for the  
U.S. DEPARTMENT OF ENERGY  
under Contract DE-AC05-84OR21400



3 4456 0283940 9



## TABLE OF CONTENTS

LIST OF TABLES . . . . .	v
LIST OF FIGURES . . . . .	vii
ABSTRACT . . . . .	1
1. INTRODUCTION . . . . .	1
1.1 PRIOR CORROSION STUDIES . . . . .	2
2. EXPERIMENTAL PROCEDURE . . . . .	5
2.1 SPECIMEN MATERIALS . . . . .	5
2.2 SPECIMEN DESIGNS . . . . .	5
2.3 CORRODANT COMPOSITION . . . . .	10
2.4 EXPOSURE TO CORRODANT . . . . .	11
2.4.1 Autoclave Tests . . . . .	11
2.4.2 Pyrex Capsule Tests . . . . .	12
2.4.3 Constant-Strain-Rate Tests . . . . .	12
2.5 EVALUATION METHODS . . . . .	17
3. RESULTS . . . . .	17
3.1 AUTOCLAVE TESTS . . . . .	17
3.2 PYREX CAPSULE TESTS . . . . .	23
3.3 CONSTANT-STRAIN-RATE TESTS . . . . .	26
4. DISCUSSION . . . . .	26
5. CONCLUSIONS . . . . .	30
6. REFERENCES . . . . .	31
APPENDIX A. WEIGHT CHANGE/DIMENSIONAL DATA DND WELD/STRESS STATUS FOR C-RING SPECIMENS USED FOR AUTOCLAVE AND CAPSULE TESTS . . . . .	33
APPENDIX B. CHP CAPSULE PREPARATION PROCEDURE . . . . .	35
APPENDIX C. CONSTANT-STRAIN-RATE TEST PROCEDURE . . . . .	37



LIST OF TABLES

Table 1. Nominal chemical composition (wt %) of the alloys investigated in chemical heat pump corrosion tests . . . . . 6

Table 2. Composition of salt mixtures used in the chemical heat pump test program . . . . . 10

Table 3. Summary of corrosion data for materials exposed to hot nitrate salt-water mixtures for 2-week test periods in stainless steel autoclaves . . . . . 19

Table 4. Chemical analysis of the corrodant removed from an autoclave after 2-week exposure of eight specimens at 250°C . . . . . 24

Table 5. Summary of corrosion data for materials exposed individually to 80% nitrate salt-20% water mixture at 250°C and 0.55 MPa . . . 25

Table 6. Chemical analyses of solutions removed from capsules after the completion of testing at 250°C . . . . . 28

Table 7. Data summary for constant-strain-rate tests run in nitrate salts at 250°C . . . . . 28



## LIST OF FIGURES

Fig. 1. Schematic of the C-ring specimen used in autoclave and capsule tests . . . . .	8
Fig. 2. An assembled and stressed C-ring specimen showing insulators and the stressing bolt . . . . .	8
Fig. 3. Exploded view of C-ring specimen hardware prior to assembly . . . . .	9
Fig. 4. Stainless steel autoclave used in exposing C-ring specimens to heated salt mixtures . . . . .	11
Fig. 5. Encapsulation stages for C-ring specimens; atypical with two specimens . . . . .	13
Fig. 6. Stainless steel jig in which encapsulated C-ring specimens were heated . . . . .	14
Fig. 7. General aspects of the constant-strain-rate apparatus used in this research . . . . .	15
Fig. 8. A tensile specimen positioned in the autoclave top of the constant-strain-rate apparatus . . . . .	16
Fig. 9. Stress-corrosion crack in specimen CP043 exposed for 2 weeks to nitrate salt at 170°C. Nital etch . . . . .	20
Fig. 10. Specimen CP043 (see Fig. 9) showing absence of cracking in fusion zone . . . . .	21
Fig. 11. Photomicrograph of specimen CP045 illustrating surface cracking as a result of a 2-week exposure in nitrate salt at 170°C. Nital etch . . . . .	21
Fig. 12. Microstructure of crack-resistant Al06B steel showing well-developed pearlite (dark) grains. Nital etch . . . . .	22
Fig. 13. Photomicrograph illustrating the formation of broad pits on the inside diameter of a 2.25Cr-1Mo tube after 2 months' exposure to nitrate salts at 250°C . . . . .	25
Fig. 14. Photomicrograph illustrating the formation of a narrow pit in the weld metal of a Monel 400 specimen after 2 months' exposure to nitrate salts at 250°C . . . . .	27



## CORROSION OF MATERIALS IN CHEMICAL HEAT PUMP WORKING FLUIDS\*

J. H. DeVan and J. S. Wolf†

### **ABSTRACT**

A series of laboratory tests were conducted to evaluate the performance of type A106B and 2.25Cr-1Mo steels, types 304 and 304L stainless steel, and the nickel-base alloy Monel 400 in chemical heat pump environments based on aqueous nitrate salt mixtures. Autoclave screening tests were initially performed to evaluate the stress corrosion cracking (SCC) properties of the materials at temperatures of 170, 210, and 250°C, respectively. In 2-week tests, one of two heats of A106B exhibited cracking tendencies, but all of the other materials showed no evidence of SCC or significant general corrosion. The cracking tendency of the susceptible steel was associated with an abnormal carbide morphology.

A series of 250°C capsule tests, conducted for times of up to 6 months, similarly indicated that neither SCC nor general corrosion was a problem area for these material-environment combinations. General corrosion rates were <0.1 mil/year (mpy). The two materials that performed best, type A106B mild steel and type 304L stainless steel, were tested while being dynamically strained in an 80% nitrate salt/20% water mixture at 250°C. These materials survived the tests with no indication of SCC or other significant corrosion effects.

Based on this relatively short-term laboratory test program, type 304L stainless steel and A106B carbon steel can be recommended as candidate classes of structural materials for the nitrate-carrying piping of the chemical heat pump. It is noted that stringent microstructural control may be required in the case of type A106B piping.

---

### **1. INTRODUCTION**

This research was conducted in support of the ORNL Chemical Heat Pump (CHP) Program, which is directing the development of high-temperature adsorption heat pumps for industrial process energy conservation. The

---

\*Research sponsored by the Waste Energy Recovery Program, Office of Industrial Programs, U.S. Department of Energy, under contract DE-AC05-84OR21400 with Martin Marietta Energy Systems, Inc.

†Permanent address: Department of Mechanical Engineering, Clemson University, Clemson, SC 29634-0921.

objective of this research was to supply preliminary, but representative, corrosion data to help determine the compatibility of candidate materials of construction for an aqueous nitrate salt working fluid at temperatures and pressures of interest. Such information is essential to the development of economic and reliable CHPs. The goal of the test program has been to provide short-term corrosion data at the screening-test level for a series of structural alloys selected as "model systems," that is, generic materials that may have potential application for high-temperature heat pumps but not necessarily the optimum compositions or microstructures of a given class, pending detailed economic and mechanical design considerations.

### 1.1 PRIOR CORROSION STUDIES

Using a computerized search program,<sup>1</sup> corrosion-rate data were located for aqueous nitrate solutions based on potassium and sodium, but no data were reported for lithium nitrate solutions. In the case of potassium nitrate solutions (10 to 90%), corrosion rates for carbon steel, 18/8 stainless steel, Monel, and 2.25Cr-1Mo steel are all listed as <20 mpy at 10 to 93°C (50–200°F). Under the same conditions, rates for these same materials in sodium nitrate solutions appear to be a factor of 10 lower (<2 mpy); however, at 121°C (250°F), rates for 18/8 stainless steel in sodium nitrate solutions (10 to 70%) are also listed as <20 mpy. Since these rates reflect maximum weight losses resulting from the combined effects of localized and general corrosion, they are useful primarily for screening out unacceptable materials rather than as a design standard. From this standpoint, the rates convey no obvious preferences among the materials previously cited. Furthermore, the data indicate that no major uniform corrosion problems should be encountered in the selected aqueous nitrate salt solutions below 100°C. Supplementary data are required for higher temperatures, however.

Although the data available for nitrate solutions suggest relatively low general and localized corrosion rates, they do not preclude the possibility of stress corrosion cracking (SCC). In fact, it is well established that certain types of plain carbon and low-alloy steels are

subject to SCC in nitrate solutions at 25 to 90°C. (Although there are no reported instances of cracking for the other material classes selected for this study, these materials have not been investigated as extensively as the ferritic steels.)

An in-depth review of the SCC of mild steels in nitrate solutions was recently published as part of a study for the Commission of the European Communities fusion reactor development program.<sup>2</sup> The following is a summary of that review (to which the reader is referred for relevant references).

Among the factors controlling SCC in carbon steels are temperature, pH, electrochemical potential, and steel composition. The temperature effect on cracking in a nitrate solution subscribes to an Arrhenius relation in which failure time is logarithmically dependent on the reciprocal of temperature, that is, failure times at a given stress decrease with increasing temperature. The temperature effect appears to be manifested through the rate of crack growth (faster at higher temperature) and not in the crack initiation time. The propensity for alkali nitrates to cause cracking increases in the order  $\text{NaNO}_3$ ,  $\text{KNO}_3$ , and  $\text{LiNO}_3$ , and may be related to the pH of these respective salt mixtures, which decreases in the order listed. The aggressiveness of  $\text{NaNO}_3$  solutions can be increased to match the other cations by decreasing the pH to that of the other cation. Conversely, the probability for SCC in a given solution can be decreased substantially as the pH is increased above about 7.

The carbon level of the steel is another critical variable affecting cracking in nitrate solutions. High-purity iron is not susceptible to SCC in nitrate environments, but, as carbon is added in the range 0.01 to 0.05%, its susceptibility goes through a maximum. Steels with above 0.25% carbon are again very resistant. This effect can apparently be traced to the location and form of carbon. When the carbon level is low, such that carbon is mainly in solution or present as small  $\text{Fe}_3\text{C}$  particles, intergranular stress corrosion is observed. As pearlite begins to form, the susceptibility diminishes. A logical explanation for this behavior is that the pearlite is not a grain boundary phase and therefore does not enhance intergranular attack. Three proposed mechanisms have been advanced for the detrimental effect of grain boundary carbon for SCC. The first is that

carbon at grain boundaries promotes the chemisorption of solute species in the nitrate solution that reduce the surface energy of microcracks.

Another model is predicated on the presumption that carbon or  $\text{Fe}_3\text{C}$  could act as a selective site for cathodic discharge. A third mechanism assumes that carbon lowers the electrode potential of grain boundaries relative to that of the adjoining grain matrix, thereby creating an active cell.

Without respect to the effects of electric potential, the SCC of mild steels in nitrate solutions can be inhibited by cathodic protection and accelerated by anodic overvoltage. (Anodic polarization also promotes intergranular corrosion of unstressed steels.) Increasing the temperature of nitrate solutions has the effect of shifting the critical anodic potential for cracking toward more negative values, thus widening the potential range over which SCC can occur.

Tests of unstressed and stressed steels in ammonium nitrate solutions indicate that at the higher ranges of anodic and cathodic overvoltages, stress has no effect on corrosion; however, at intermediate anodic overvoltages, a significant increase in current density is produced by stress. Stress also shifts the regions of passivity to more positive potentials. If the times to failure in stress tests are correlated with polarization potential and current density, the highest susceptibility to SCC is found at the transition between active anodic corrosion and passive film formation. In constant-strain-rate tests of mild steel in sodium nitrate solutions at  $102^\circ\text{C}$  at two pH levels (10.3 and 4.8), current density increased as a direct function of the total strain and the increase in potential (above the corrosion potential) at each pH.

The same report<sup>2</sup> that presented the aforementioned review also provides preliminary experimental data on the comparative corrosion behavior of stainless steels in lithium nitrate solutions at 95 and  $250^\circ\text{C}$ . Potentiodynamic polarization tests were conducted on both type 316 austenitic stainless steel and a high-chromium martensitic steel (DIN 1.4914) at two salt concentration levels 2.9 wt % and 28.7 wt %. At  $95^\circ\text{C}$ , the anodic currents were extremely low for both steels, and passive behavior was observed for almost the entire potential range above the corrosion potential. No significant differences were noted between the two salt concentration levels. Increasing the temperature to  $250^\circ\text{C}$  resulted in

a 1- to 2-order-of-magnitude increase in current density at both salt concentrations; and in the passive range, there are abrupt changes in current with increasing potential, suggesting that more than one surface reaction can be operative at elevated temperatures. The researchers conclude from these studies that no major uniform corrosion problems are indicated, and no visible corrosion effects were discernible on the specimens after testing. However, the tests did not address the issue of localized corrosion, which the researchers plan to examine in future tests.

## 2. EXPERIMENTAL PROCEDURE

The test program involved the exposure of five candidate CHP materials to aqueous mixtures of three nitrate salts ( $\text{NaNO}_3$ ,  $\text{KNO}_3$ , and  $\text{LiNO}_3$ ) at elevated temperature and pressure. In order to monitor a broad scope of potential corrosion behaviors, three distinctly different types of tests were utilized: autoclave tests, capsule tests, and constant-strain-rate tests. The details of these testing methods are further described.

### 2.1 SPECIMEN MATERIALS

Five alloys commonly used in pressurized piping systems at the temperatures of interest were selected for investigation: type A106B carbon steel, Grade T3 2.25Cr-1Mo alloy steel, types 304 and 304L stainless steel, and Monel 400 (a nickel-base alloy). The typical compositions of these materials are shown in Table 1.

### 2.2 SPECIMEN DESIGNS

A C-ring specimen design\* was used in both the autoclave tests and the capsule tests and is illustrated schematically in Fig. 1. Specimens of all five alloys were fabricated from pipe stock by off-site machine shops.

---

\*Specimen design conforms to American Society for Testing and Materials (ASTM) standard recommended practices as defined in ASTM Standard G38-73.

Table 1. Nominal chemical composition (wt %) of the alloys investigated in chemical heat pump corrosion tests

Element	Alloys				
	A106B <sup>a</sup>	2.25Cr-1Mo Gr. T3 <sup>a</sup>	304 <sup>b</sup>	304L <sup>b</sup>	Monel 400 <sup>b</sup>
C	0.30	0.15	0.08 max	0.03 max	0.30 max
Cr		1.65-2.35	19.0	19.0	
Mn	0.29-1.06	0.30-0.60			2.0 max
Mo		0.44-0.65			
Si	0.10 min	0.50 max			0.50 max
S	0.058 max	0.030 max			0.24 max
P	0.048 max	0.030 max			
Fe	Balance	Balance	Balance	Balance	2.5 max
Ni			10.0	10.0	63.0-70.0
Cu					Balance

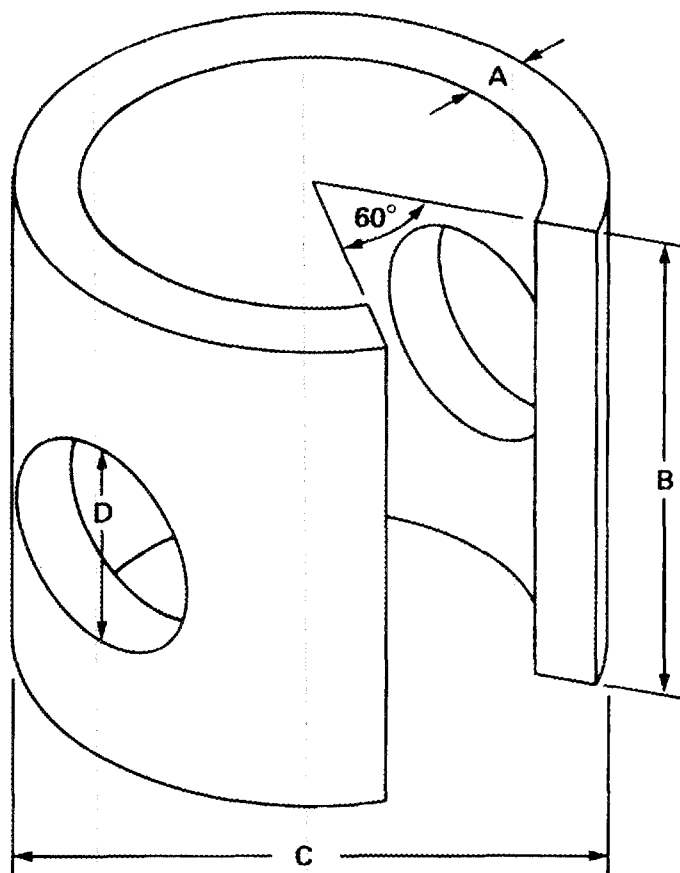
<sup>a</sup>ASM Metals Handbook, Vol. 1, 9th ed., 1978.

<sup>b</sup>ASM Metals Handbook, Vol. 3, 9th ed., 1980.

For each alloy, two modifications of this specimen design were produced: (1) an unaltered or seamless specimen and (2) a specimen with an autogenous seam weld in the longitudinal direction of the pipe and opposite the 60° opening. The purpose of these latter specimens was to simulate the effect of welds in CHP systems. Subsequent to their receipt and cleaning, the linear dimensions, area, and initial mass of each specimen were determined in order to facilitate the later evaluation of their corrosion resistance. A listing of these measurements together with the assigned specimen numbers and after-test weights is given in Appendix A.

To prepare the C-ring specimens for corrosion testing, a stainless steel bolt fitted with Teflon insulators was inserted through the holes of the C-ring and tightened such that the outer arc of the vee opening (Fig. 1) was reduced by 1.3 mm (0.050 in.). This operation ensured that the material opposite the opening was stressed to its yield point, thus providing the stress necessary to drive the SCC process if such was inherent to the alloy-corrodant system. The purpose of the Teflon insulators was to provide electrical insulation between the C-ring and the stainless steel bolt so as to avoid galvanic effects between the metallic

ORNL-DWG 88-6637A



A = 1.5 mm (0.06 in.)  
B = 12.7 mm (0.50 in.)  
C = 12.7 mm (0.50 in.)  
D = 6.4 mm (0.25 in.)

Fig. 1. Schematic of the C-ring specimen used in autoclave and capsule tests.

components of the assembly. An assembled view of the stressed C-ring is shown in Fig. 2, while a typical exploded view is illustrated in Fig. 3.

The second type of specimen design used in this research was a subsized tensile specimen, having a gage length of 50.8 mm (2 in.), a diameter of 3.2 mm (0.125 in.), and an overall length of 101.6 mm (4 in.). Such specimens were used in conjunction with the constant-strain-rate tests discussed later. These specimens were machined from thick-wall pipe stock

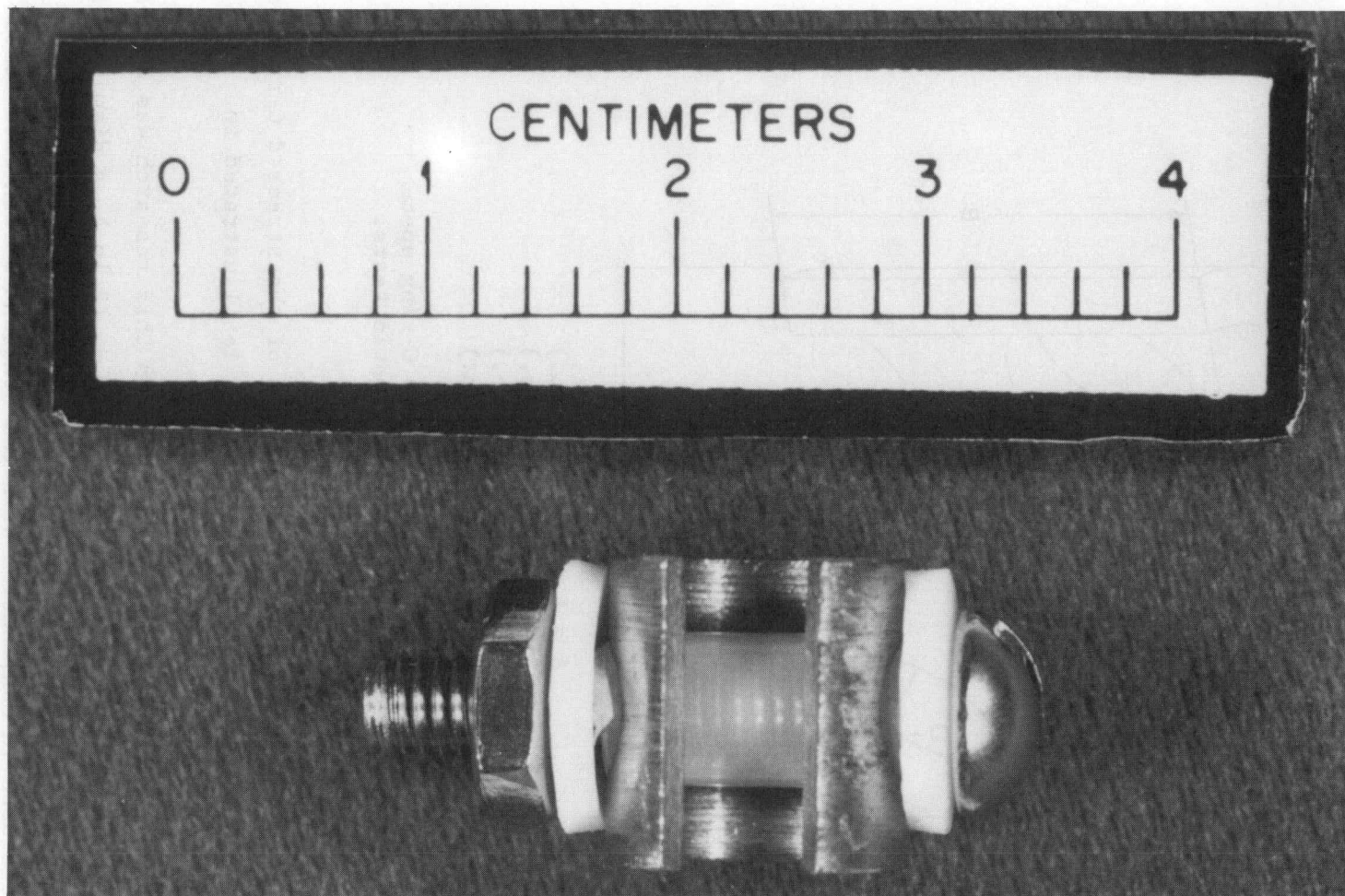


Fig. 2. An assembled and stressed C-ring specimen showing insulators and the stressing bolt.

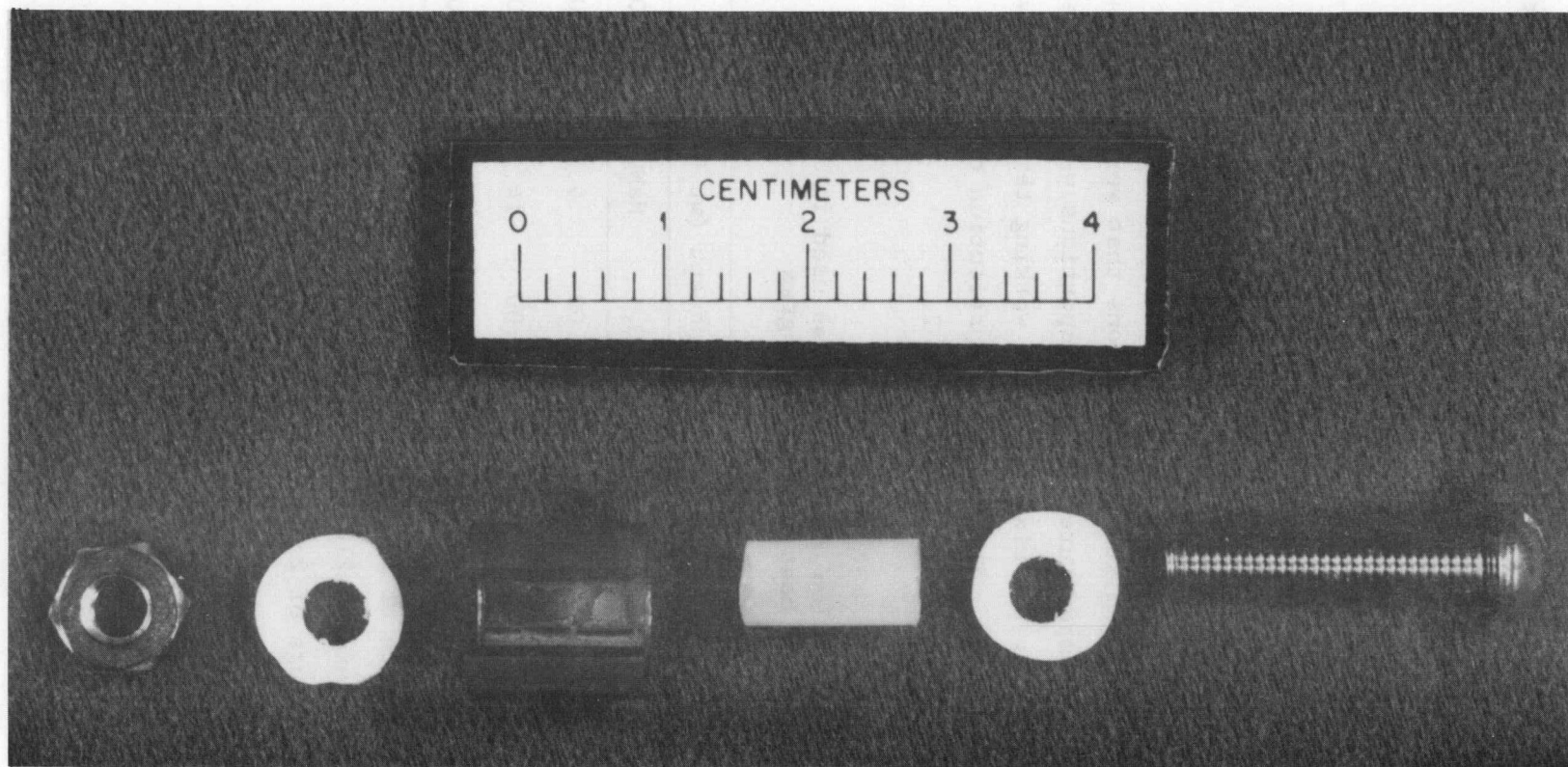


Fig. 3. Exploded view of C-ring specimen hardware prior to assembly.

by vendors external to ORNL. Prior to their use, the gage-length dimensions were measured to the nearest 20  $\mu\text{m}$  in order to later determine the axial strain resulting from the testing procedure.

### 2.3 CORRODANT COMPOSITION

The corrodants used in this testing program were a series of three working fluid mixtures intended for use in adsorption-type heat pumps. The mixtures consisted of distilled water as the volatile constituent and reagent-grade nitrate salts ( $\text{LiNO}_3$ ,  $\text{KNO}_3$ , and  $\text{NaNO}_3$ ) as the nonvolatile constituent, all of which were admixed in proportions that were dependent on the intended use or test temperature. These proportions were adjusted so that the vapor pressure over the mixture at the working temperature was  $\sim 0.55$  MPa (5.5 bar) in each case. The detailed constitution of these working fluid-corrodant mixtures is given in Table 2.

Table 2. Composition of salt mixtures used in the chemical heat pump test program

Mixture	Component (wt %)			
	$\text{LiNO}_3$	$\text{KNO}_3$	$\text{NaNO}_3$	$\text{H}_2\text{O}$
50% nitrate salts-50% water <sup>a</sup>	26.50	14.00	9.50	50.00
75% nitrate salts-25% water <sup>b</sup>	39.75	21.00	14.25	25.00
80% nitrate salts-20% water <sup>c</sup>	42.40	22.40	15.20	20.00

<sup>a</sup>Intended use temperature of 170°C.

<sup>b</sup>Intended use temperature of 210°C.

<sup>c</sup>Intended use temperature of 250°C.

## 2.4 EXPOSURE TO CORRODANT

### 2.4.1 Autoclave Tests

For the purpose of preliminary and rapid screening of the candidate alloys in the corrodant, stainless steel autoclaves were used so that many different types of specimens could be exposed simultaneously. The autoclave had an internal diameter of 34.9 mm (1-3/8 in.) and an overall length of 0.3 m (12 in.). Figure 4 shows the device with its associated thermocouple and valving.

YP 5147

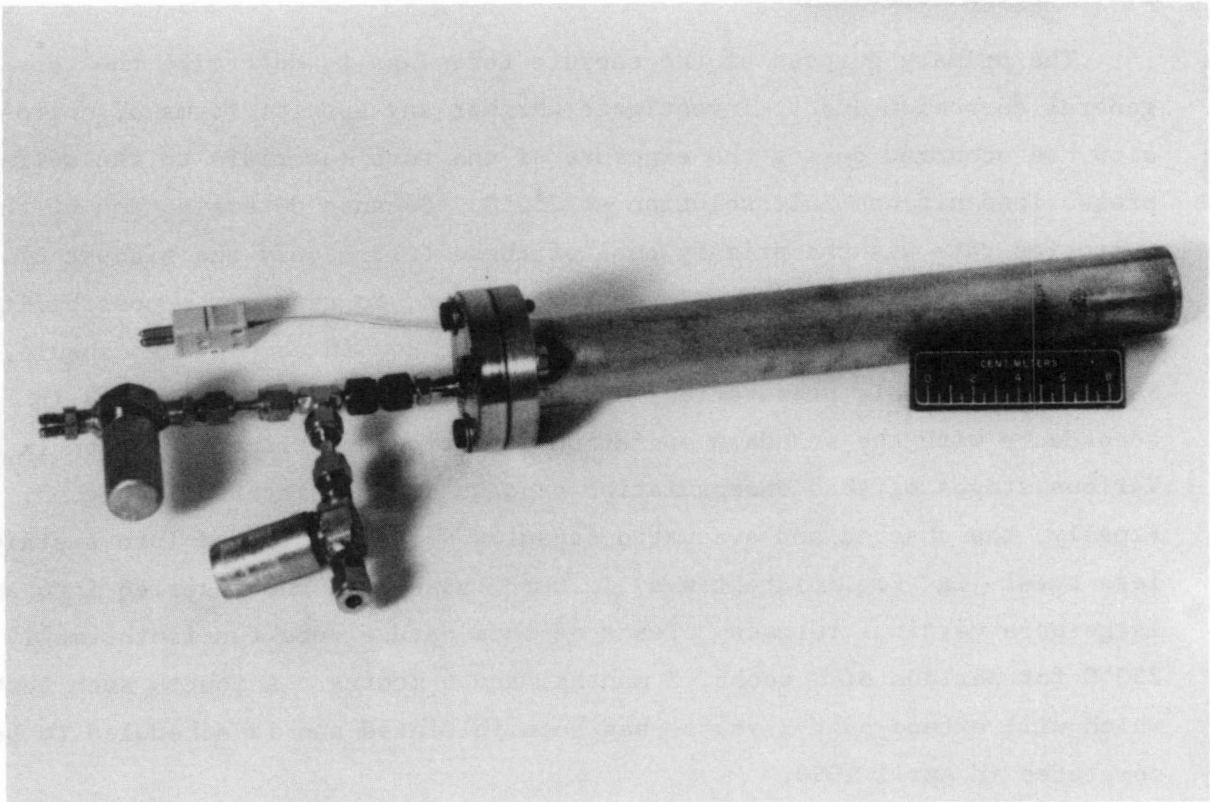


Fig. 4. Stainless steel autoclave used in exposing C-ring specimens to heated salt mixtures.

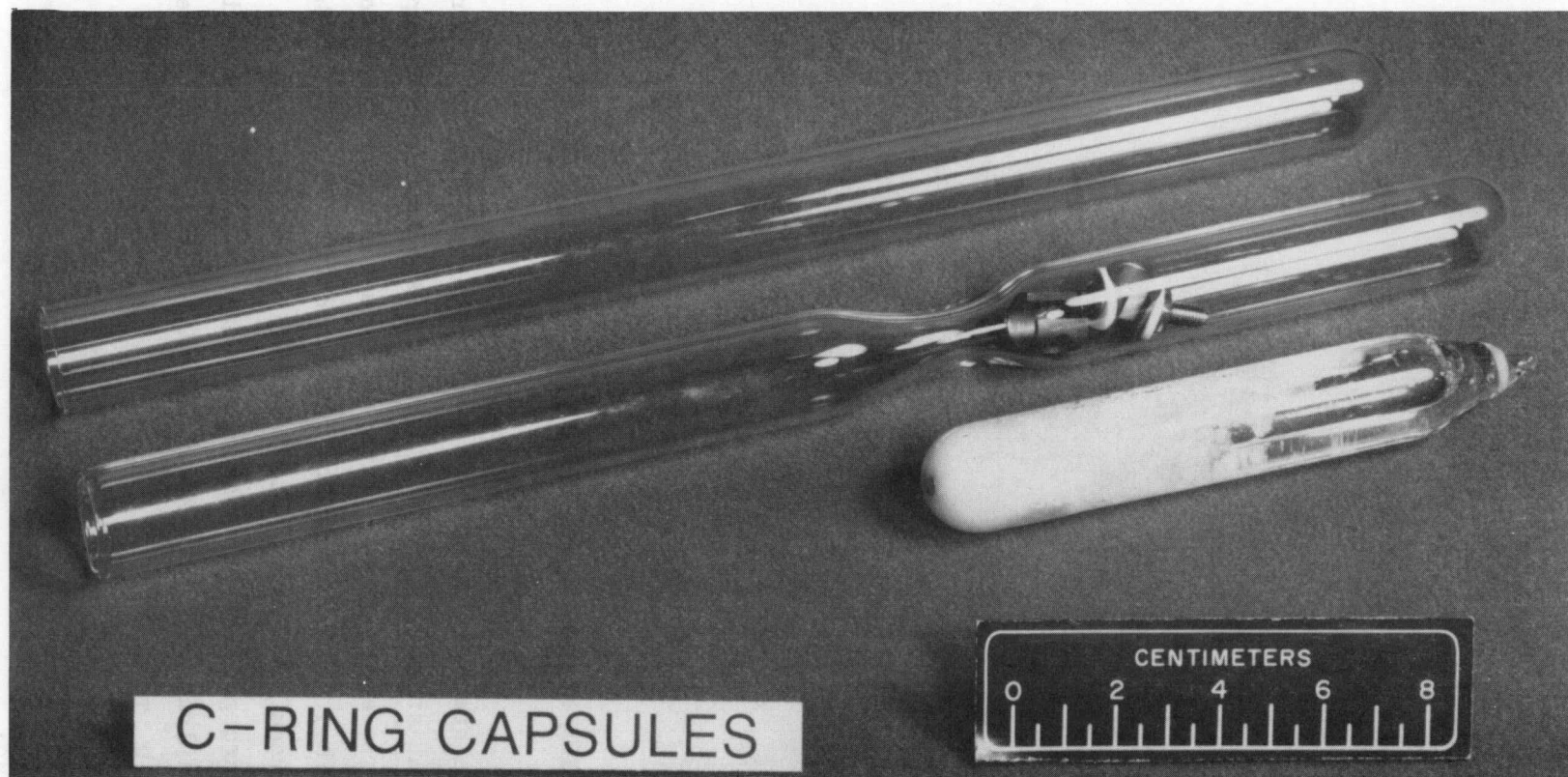
The autoclave, after being partially filled with corrodant, is loaded with a "string" of C-ring specimens that are supported from a single Teflon rod fixed to the cap of the autoclave. For most tests, the specimens were fully immersed in the corrodant; however, in one instance, half of the specimens were immersed in fluid, whereas the remaining specimens were exposed to the vapor phase above it. Subsequent to specimen insertion, the autoclave was sealed and evacuated with a roughing pump for ~5 min in order to minimize oxygen contamination of the salt mixture. Finally, after such preparation, the charged autoclaves were inserted into vertical furnaces and held isothermally for a period of 2 weeks. Such tests were conducted at temperatures of 170, 210, and 250°C.

#### 2.4.2 Pyrex Capsule Tests

The primary purpose of the capsule tests was to determine the rate of general corrosion and to investigate whether any special forms of corrosion had occurred during the exposure of the test materials to the self-pressurized nitrate salt solution at 250°C. Because determination of the corrosion rate was the primary goal of these tests, only the highest of the temperatures of interest was investigated; and, to reduce the possibility of data distortion, only one specimen was exposed in each pyrex capsule. Subsequent to their preparation, C-ring specimens were encapsulated in accordance with the standard operational procedure outlined in Appendix B. Various stages of that encapsulation process are illustrated in Fig. 5. Finally, the charged and evacuated capsules were then loaded into a stainless steel jig (Fig. 6) that was, in turn, assembled and inserted into a large-bore vertical furnace. Tests of this nature were run isothermally at 250°C for periods of 2 weeks, 2 months, and 6 months. A fourth such test, which will extend over 2 years, has been initiated and is scheduled to be completed in April 1990.

#### 2.4.3 Constant-Strain-Rate Tests

The primary purpose of the constant-strain-rate tests was to determine whether dynamic mechanical deformation might destroy the integrity of some protective surface film and thereby lead to an early SCC-related failure of the test materials. Subsize tensile specimens of the two more promising



C-RING CAPSULES

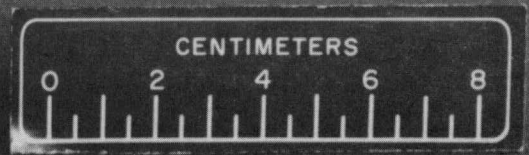
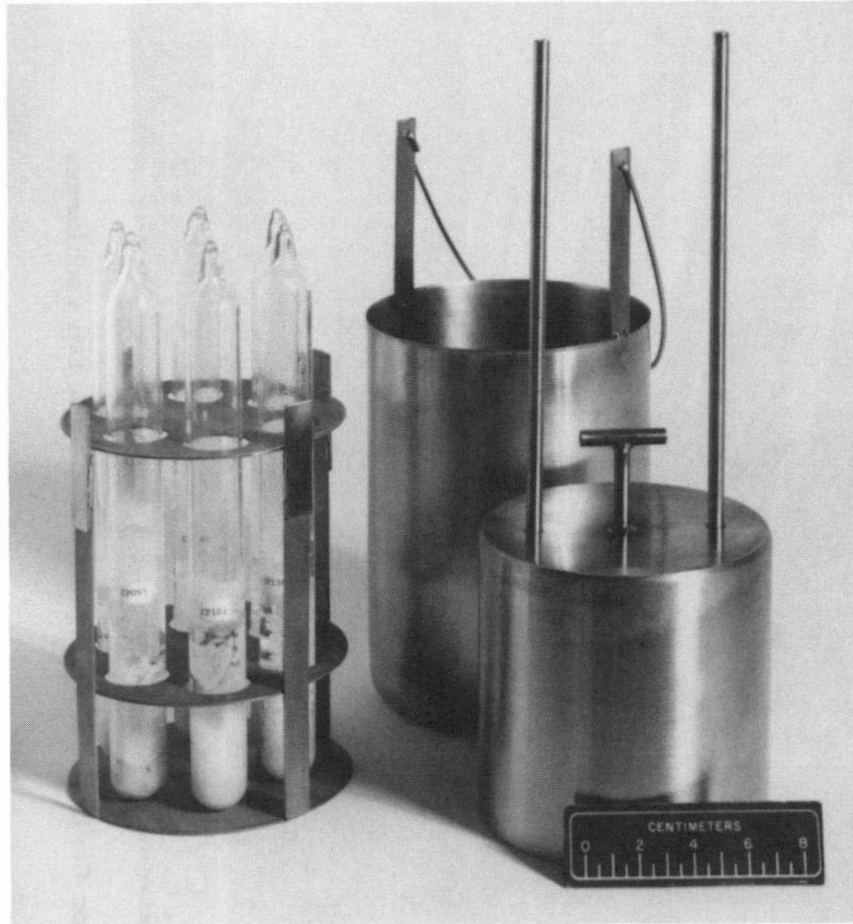
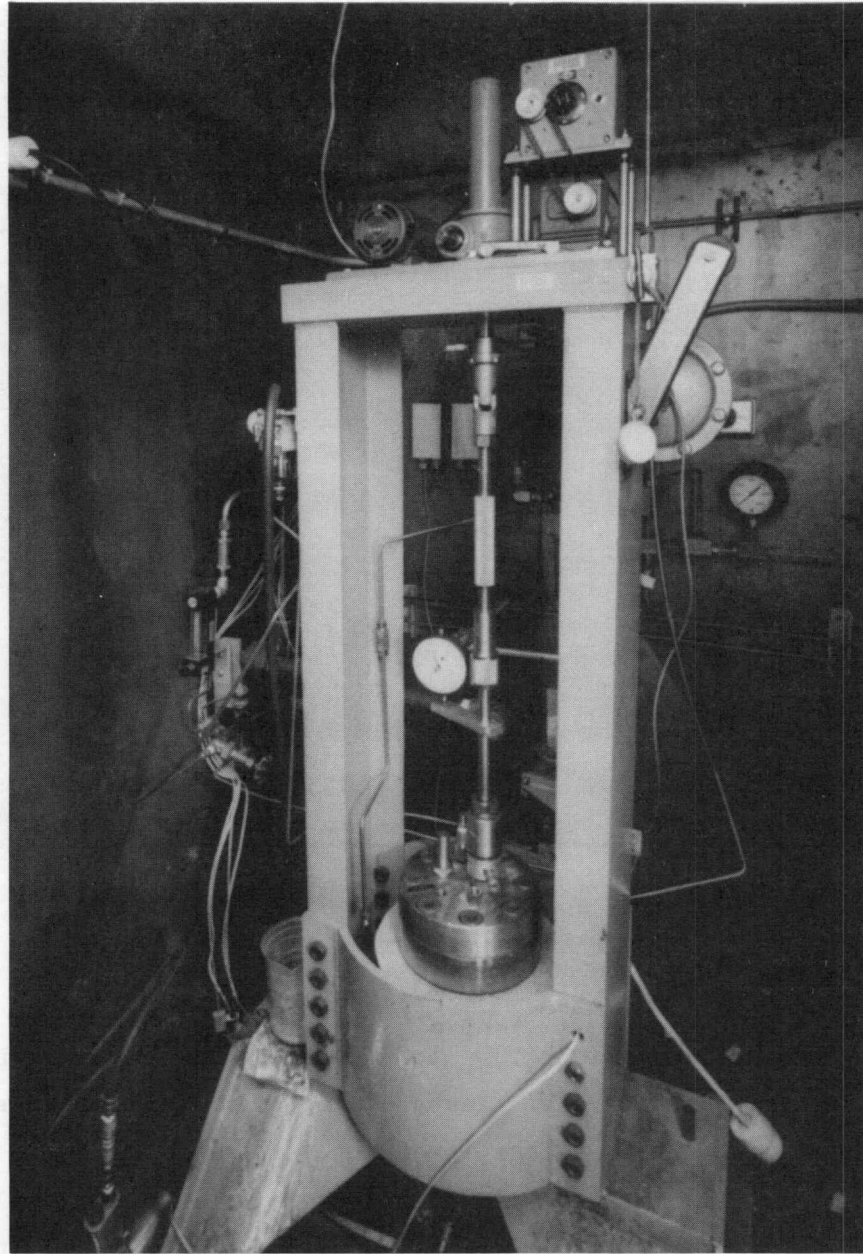


Fig. 5. Encapsulation stages for C-ring specimens; atypical with two specimens.



**Fig. 6. Stainless steel jig in which encapsulated C-ring specimens were heated.**

materials, type 304L stainless steel and type A106B carbon steel, were tested under constant-strain conditions using the specially built apparatus shown in Fig. 7. This equipment consisted of a custom-built frame housing a 165-mm-diam (6.5-in.) vertical furnace into which was fitted a high-pressure autoclave manufactured by Autoclave Engineers, Incorporated. A pull rod, passing through a seal in the demountable top of the autoclave, was driven through a load cell by a Model P-2000 variable-speed drive manufactured by the W. T. Specialty Company. This drive, shown atop the load frame in Fig. 7, is discretely variable by gear ratio selection and is essentially continuously variable via the use of a Minarik motor speed controller (not shown).



**Fig. 7. General aspects of the constant-strain-rate apparatus used in this research.**

The tensile specimen was first mounted within the gripping device, which is integral with the autoclave top (Fig. 8). The standard operating procedure outlined in Appendix C was then followed in carrying out the constant-strain tests. Both materials were tested at 250°C at crosshead

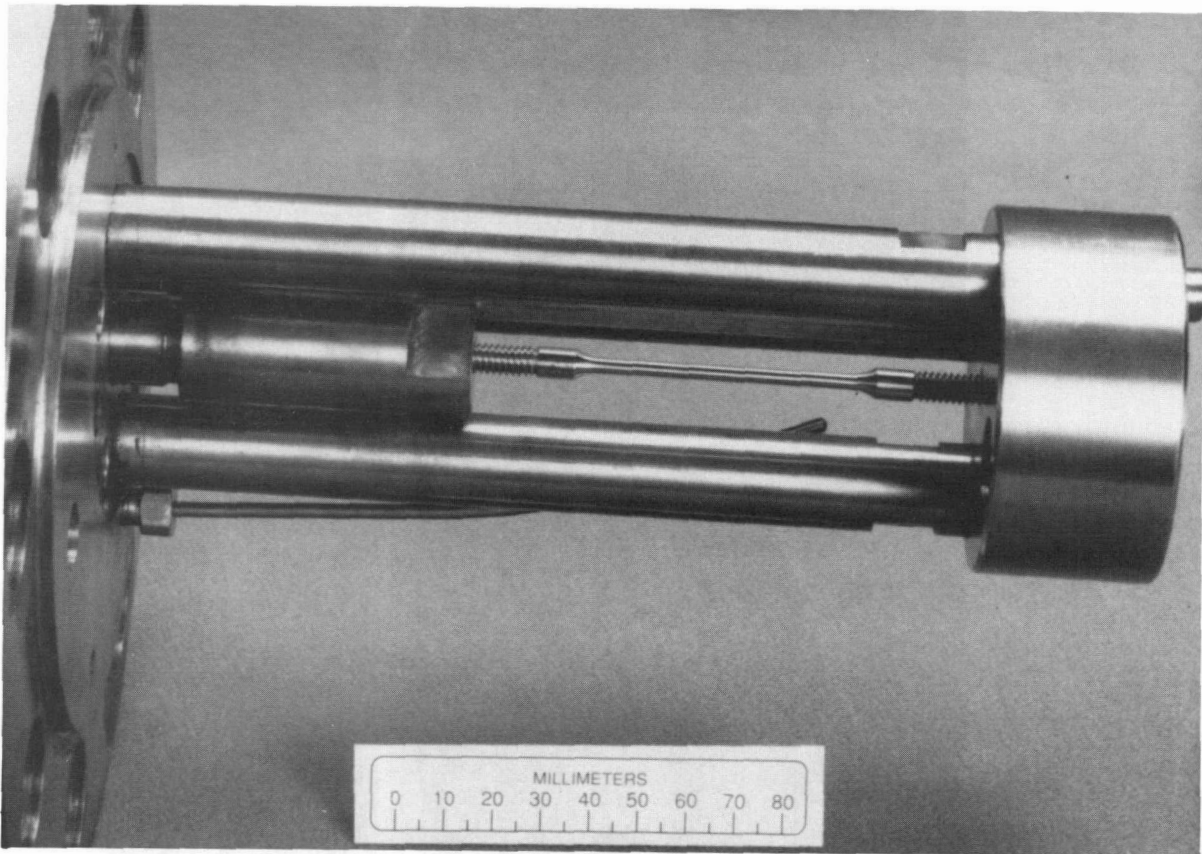


**Fig. 8. A tensile specimen positioned in the autoclave top of the constant-strain-rate apparatus.**

drive rates of  $3.3 \mu\text{m}/\text{min}$  ( $1.3 \times 10^{-4}$  in./min) and  $7.9 \mu\text{m}/\text{min}$  ( $3.1 \times 10^{-5}$  in./min), respectively. Tests at the higher strain rate had a duration of ~20 h, and, at the lower rate, which represented the lower limit of crosshead velocity obtainable, had a duration of ~65 h each. Since the gage length of the specimens was 50.8 mm (2 in.), the strain rates imposed by these tests were  $\sim 6.7 \times 10^{-5}/\text{min}$  and  $1.6 \times 10^{-5}/\text{min}$ , respectively. The strain rates were selected to achieve total strains in excess of 5% of the gage length, with exposure under corrosive conditions of at least 20 h.

## 2.5 EVALUATION METHODS

Subsequent to their exposure, the C-ring specimens were cleaned and reweighed in order to determine the mass losses incurred. From these determinations, specific mass losses ( $\text{mg}/\text{cm}^2$ ) and average general corrosion rates, in terms of wastage in mils per year (mpy), were calculated. All specimens were subjected to microscopic examination, with special attention given to the possible presence of localized forms of corrosion such as pitting or SCC. In addition, representative specimens were inspected and photographed using the standard techniques of optical metallography. Finally, corrodant solutions from the longer-term tests were chemically analyzed both prior and subsequent to their use in this research. These analyses had three objectives: (1) to verify the starting nitrate salt concentrations; (2) to determine the levels of trace impurities in the salts prior to testing, as well as impurities acquired from test components other than the specimens; and (3) to evaluate the solute concentrations of the major constituents of the test specimens at the end of testing.

In one instance of anomalous material behavior, several sophisticated techniques were employed in an attempt to determine the cause of the anomaly. These methods included optical metallography coupled with special heat treatments, energy-dispersive spectroscopy, specialized chemical analyses, and an electron microprobe analysis.

## 3. RESULTS

### 3.1 AUTOCLAVE TESTS

The primary purpose of the autoclave tests was to rapidly screen all the alloys with regard to their propensity for SCC using the nitrate mixtures and test temperatures detailed in Table 2. Although corrosion-rate data are also available for these tests, they are judged to be somewhat less reliable than those secured from the capsule tests (Sect. 3.2)

because of the possibility of cross-contamination effects. At the lower temperatures, these tests contained the full complement of five material types; however, for the 250°C test, the Monel was not tested because of a delay in procurement. [Monel was investigated in the 250°C capsule tests (Sect. 3.2).]

A summary of the autoclave test data is presented in Table 3. Although all of these tests contained equal numbers of welded and seamless specimens, they are not differentiated because their corrosion behavior was similar. Specimens in all cases exhibited a net weight loss, which was used as the basis for the corrosion rates in Table 3. Exposed surfaces darkened slightly during the test, but corrosion-product scales were extremely superficial. Inspection of the data in Table 3 indicates that, as may have been expected, the degree of general corrosion increases with increasing test temperature for most of the materials tested. The stainless steels are an exception to this generalization, most probably because of their propensity to form extremely passive corrosion-product films at all temperatures.

The worst of the materials problems encountered involved the cracking of one (and only one) batch of type Al06B steel specimens. This phenomenon occurred in both the liquid and vapor phase above the nitrate salt mixture at 170°C. Cracking was intergranular, as shown in Fig. 9, and did not occur in the fusion zone of the welded specimens (see Fig. 10). To rule out the possible effects of cross contamination from dissimilar alloys, a confirmation test was run at 170°C using a single encapsulated specimen of the affected Al06B; cracking was again noted. A photomicrograph of this specimen, illustrating what is apparently SCC behavior, is shown in Fig. 11. Note that the cracks appear to have emanated from the base of previously formed corrosion pits. The typical microstructure of the crack-resistant Al06B heats is shown in Fig. 12. The major difference is the presence of well-developed pearlite grains (dark constituent) in the latter heats and the absence of definable pearlite grains in the susceptible heats (see Fig. 10). The microstructure of the resistant heats typifies that

**Table 3. Summary of corrosion data for materials exposed to hot nitrate salt-water mixtures for 2-week test periods in stainless steel autoclaves**

Material type	Specimen	Specific mass loss (mg/cm <sup>2</sup> )	Corrosion rate (mpy)	Remarks
<b>170°C tests; vapor-phase exposure</b>				
A106B	CP037	0.101	0.132	Cracked <sup>a</sup>
A106B	CP042	0.076	0.100	Cracked <sup>a</sup>
A106B	CP089	0.015	0.020	b
A106B	CP094	0.032	0.042	b
Cr-Mo	CP047	0.063	0.083	
Cr-Mo	CP052	0.088	0.115	b
304 SS	CP057	0.075	0.096	
304 SS	CP062	0.063	0.081	b
304L SS	CP078	0.025	0.032	
304L SS	CP083	0.025	0.032	b
Monel 400	CP068	0.050	0.059	
Monel 400	CP073	0.089	0.103	b
<b>170°C tests; liquid-phase exposure</b>				
A106B	CP038	0.076	0.099	Cracked <sup>a</sup>
A106B	CP043	0.126	0.165	Cracked <sup>a</sup>
A106B	CP088	0.017	0.022	
A106B	CP093	0.151	0.197	b
Cr-Mo	CP048	0.113	0.149	
Cr-Mo	CP053	0.076	0.099	b
304 SS	CP058	0.075	0.096	
304 SS	CP063	0.038	0.048	b
304L SS	CP079	0.013	0.016	
304L SS	CP084	0.025	0.032	b
Monel 400	CP069	0.038	0.044	
Monel 400	CP074	nil	nil	b
<b>210°C tests; liquid-phase exposure</b>				
A106B	CP113	0.119	0.155	b
A106B	CP118	0.109	0.142	b
Cr-Mo	CP050	0.218	0.285	b
Cr-Mo	CP102	0.215	0.282	b
304 SS	CP059	0.098	0.126	b
304 SS	CP066	0.060	0.077	b
304L SS	CP080	0.080	0.063	b
304L SS	CP137	0.021	0.027	b
Monel 400	CP070	0.199	0.232	b
Monel 400	CP109	0.121	0.140	b
<b>250°C tests; liquid-phase exposure</b>				
A106B	CP001	0.837	1.094	Small pits
A106B	CP006	0.407	0.531	b
Cr-Mo	CP010	1.624	2.127	b
Cr-Mo	CP015	1.128	1.478	Pitting
304 SS	CP019	0.0126	0.016	b
304 SS	CP023	0.038	0.048	b
304L SS	CP028	0.038	0.048	Small pits
304L SS	CP034	0.025	0.032	b

<sup>a</sup>Anomalous batch of A106B material.

<sup>b</sup>No cracks or pits noted in stressed specimen.

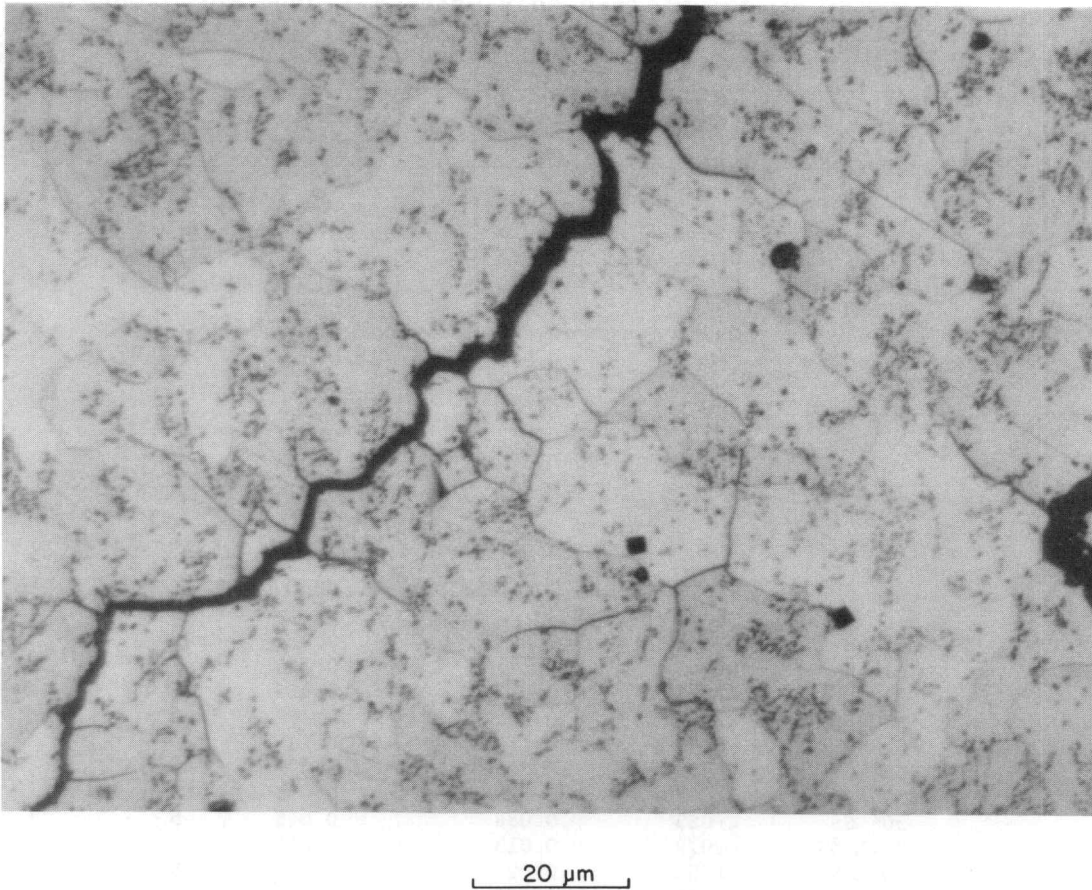
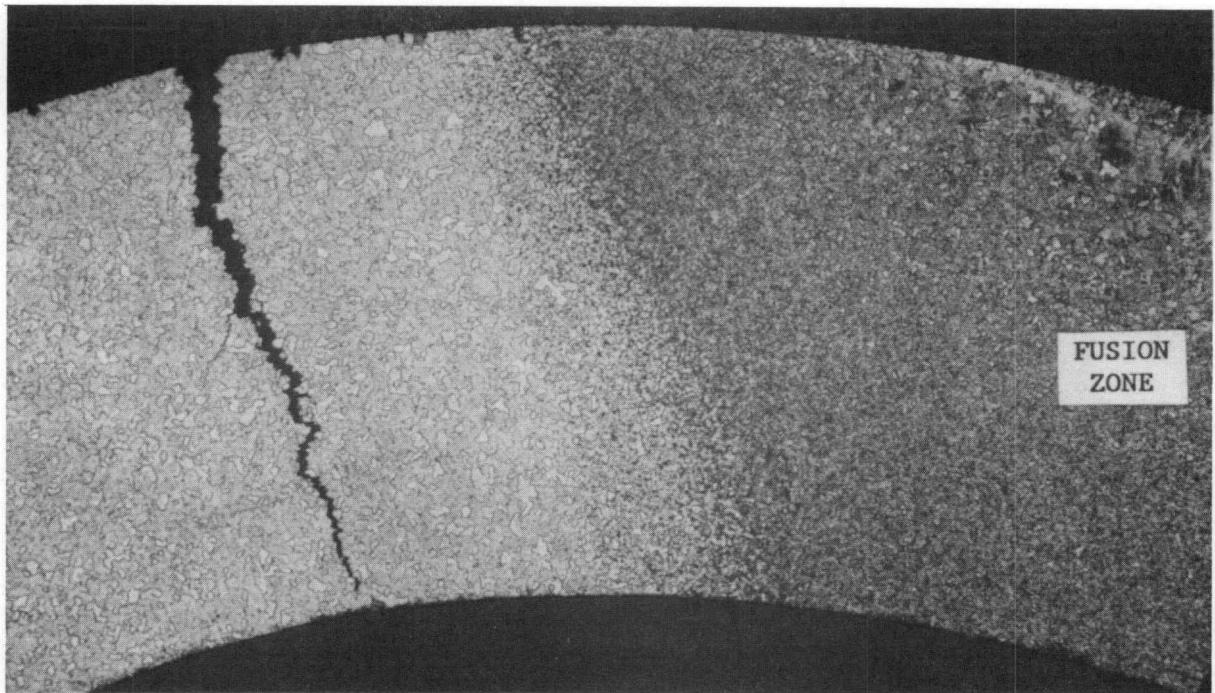


**Fig. 9. Stress-corrosion crack in specimen CP043 exposed for 2 weeks to nitrate salt at 170°C. Nital etch.**

normally associated with Al06B, whereas that of the susceptible heats is more anomalous. It was this observation that prompted a deeper investigation of the one lot of Al06B which exhibited this structure.

Since SCC is in many instances associated with the presence of halides in the corrodant, and since we had used fluorine-containing Teflon insulators with the specimens, the fluorine content of the salt solution was analyzed. The fluorine concentration of the solution after testing was found to be less than that contained as an impurity in the reagent salts (440 ppm). It was therefore concluded that the Teflon was stable under the test conditions and that it was not contributory to failure. Chemical analyses of the susceptible Al06B heat showed the steel to conform to ASTM

Y209543



400 μm

Fig. 10. Specimen CP043 (see Fig. 9) showing absence of cracking in fusion zone.

Y209862



40 μm

Fig. 11. Photomicrograph of specimen CP045 illustrating surface cracking as a result of a 2-week exposure in nitrate salt at 170°C. Nital etch.

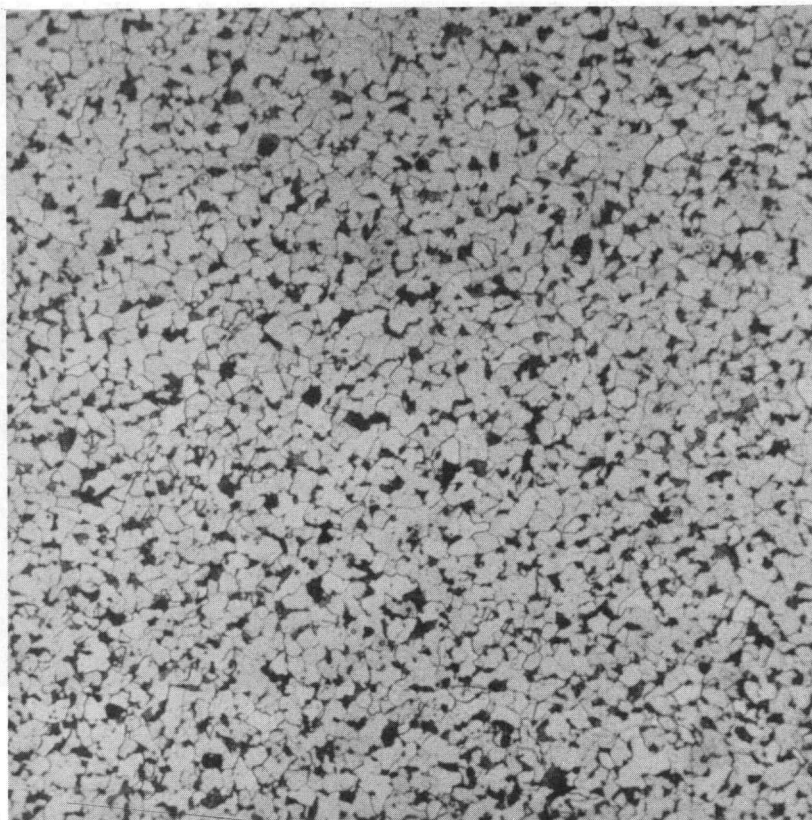


**Fig. 12. Microstructure of crack-resistant A106B steel showing well-developed pearlite (dark) grains. Nital etch.**

standard chemical requirements with respect to carbon and residual metal concentrations. (The carbon level of the susceptible heat was analyzed to be 0.020%.) Subsequent specialized analyses of the steel (including an electron probe microanalysis for possible grain boundary segregation of the light elements boron, nitrogen, and oxygen) also failed to indicate any unusual elemental presence that might lead to SCC. Given the carbon level of the susceptible heat, its microstructure would normally be expected to exhibit identifiable pearlite grains such as those in Fig. 12. In fact, a normalizing heat treatment of the susceptible heat did produce a microstructure similar to that of Fig. 12. Neither a normalizing nor spheroidizing heat treatment was effective in reproducing the microstructure in

Fig. 9, therefore its thermal history remains an uncertainty. In summary, the cause of SCC in the A106B material can be traced to the unusual microstructure of the affected heat, that is, carbides in a form different from pearlite. However, the heat treatment that led to this microstructure remains undefined. We conclude that some type of "sensitized" A106B does exist in commerce and that the best mode known to us for its detection is the application of metallographic inspection as a quality assurance technique.

With the one exception cited above, none of the materials exhibited SCC at any of the three temperatures investigated. The 2.25Cr-1Mo steel and, to a much smaller extent, the type 304 stainless steel did exhibit a slight degree of surface pitting.

Chemical analyses of the corrodant subsequent to testing verified the salt concentrations used and indicated that relatively small amounts of the structural metallic or specimen metals had been taken into solution (see Table 4). However, as the autoclave body itself was fabricated of stainless steel, it is not possible to accurately partition the analysis in a manner that would allow determination of the fraction of concentration changes arising from the specimens themselves.

### 3.2 PYREX CAPSULE TESTS

The primary purpose of the capsule tests was to determine the rate of general corrosion and to investigate whether any special forms of corrosion had occurred during the exposure of the test materials to the self-pressurized nitrate salt solution at 250°C. These tests also provided information regarding the longer-term propensity for SCC in the 80% salt mixture only at 250°C. Tests of the pyrex encapsulation technique indicated that this glass had adequate stability in both the mechanical and chemical senses at 250°C. Mechanically, the pyrex afforded adequate strength, provided the end seal was fully developed. Chemically, there was no visual indication of surface etching or discoloration of the pyrex, and in qualification tests, the silicon concentration in the corrodant salt-water mixture showed no significant change ( $\leq 10$  ppm) as a result of a 1-week exposure at 250°C.

**Table 4. Chemical analysis of the corrodant removed from an autoclave after 2-week exposure of eight specimens at 250°C**

Element	Concentration (mg/20 mL)
<b>Elements of the corrodant salt phase</b>	
Potassium	3200
Lithium	1300
Sodium	1300
<b>Elements representative of the metal phase</b>	
Chromium	0.32
Iron	0.07
Nickel	<0.06
Molybdenum	<0.04

Corrosion-rate data for the specimens subjected to this test are summarized in Table 5. Of all the specimens tested, none exhibited SCC failures except those of the anomalous lot of type A106B material previously discussed. A retest of another heat of that same material (2-week test period) showed no evidence for SCC, nor did this material crack during longer exposures. In most cases, the rate of the corrosion was small for all materials, usually <0.1 mpy and in many cases <0.01 mpy. Such low rates appear to be acceptable for the intended CHP application.

Some materials-related problems not associated with SCC failure were noted in these tests. For example, in the 2-month tests, the 2.25Cr-1Mo steel exhibited pitting and a commensurately large weight loss in comparison with other alloys. The propensity for this alloy to pit had also been noted in the autoclave tests, and that effect is clearly evident in the photomicrograph shown in Fig. 13. This type of behavior usually contraindicates the use of a material, since the pitting process can in many cases lead either to tube perforation or to other and more drastic corrosion effects (as SCC) in long-term applications. A second and somewhat less severe form of pitting was observed in the weld metal of a

**Table 5. Summary of corrosion data for materials exposed individually to 80% nitrate salt-20% water mixture at 250°C and 0.55 MPa**

Material type	Specimen	Specific mass loss (mg/cm <sup>2</sup> )	Corrosion rate (mpy)	Remarks
<b>Two-week test period</b>				
Al06B	CP039	0.0126	0.0165	Anomalous lot
Al06B	CP044	0.0254	0.0332	Anomalous lot
Al06B	CP092	0.0607	0.0793	
Cr-Mo	CP049	0.0381	0.0499	
Cr-Mo	CP055	0.0756	0.0990	
304 SS	CP056	0.0504	0.0644	
304 SS	CP061	0.0630	0.0806	
304L SS	CP077	0.0252	0.0322	
304L SS	CP082	nil	nil	
Monel 400	CP067	0.0381	0.0443	
Monel 400	CP072	nil	nil	
<b>Two-month test period</b>				
Al06-B	CP090	0.0597	0.0182	
Al06-B	CP095	0.0834	0.0254	
Cr-Mo	CP101	0.203	0.0621	Pitted
304 SS	CP065	0.0340	0.0101	
304-L SS	CP136	0.0198	0.0059	
Monel-400	CP076	0.0328	0.0089	
<b>Six-month test period</b>				
Al06B	CP086	0.0640	0.0065	Filmed
Al06B	CP091	0.0917	0.0093	Filmed
Cr-Mo	CP054	0.1021	0.0104	Filmed
304 SS	CP064	0.0718	0.0071	Bright
304L SS	CP085	nil	nil	Bright
Monel 400	CP075	0.0292	0.0026	Filmed

Y210944

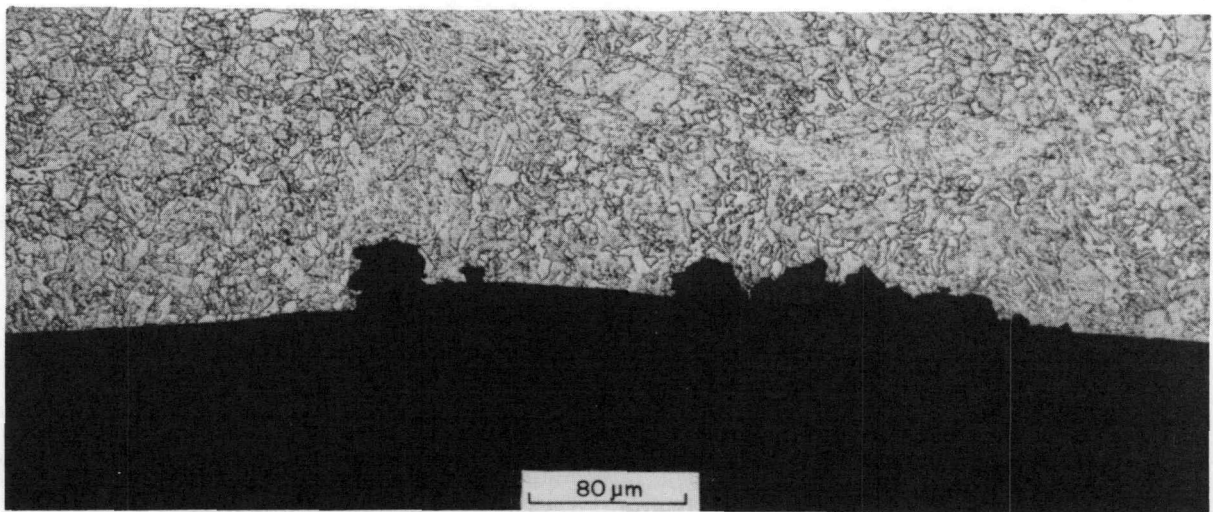


**Fig. 13. Photomicrograph illustrating the formation of broad pits on the inside diameter of a 2.25Cr-1Mo tube after 2 months' exposure to nitrate salts at 250°C.**

Monel 400 specimen that had been similarly exposed (see Fig. 14). Because these specimens have shown some propensity for pitting, and because they are more expensive materials than the Al06B steel, they are not recommended first choices for CHP components.

Selected solutions were extracted from these capsule tests and were analyzed for the presence of dissolved elements that would have come both from the specimens (iron, chromium, nickel, and molybdenum) and from the capsule itself (silicon). The results of those analyses are summarized in Table 6.

### 3.3 CONSTANT-STRAIN-RATE TESTS

The primary purpose of the constant-strain-rate tests was to determine whether dynamic mechanical deformation might destroy the integrity of some protective surface film and thereby lead to an early SCC-related failure of the test specimens. Two materials, type Al06B and type 304L stainless steel, were run at each of two strain rates in the 80% nitrate salt-20% water mixture at 250°C. Neither SCC nor any other evidence for brittle behavior was noted with either type of specimen. Details of the tests results are summarized in Table 7. As is evident from this ductile behavior under very aggressive test conditions, these materials are resistant to SCC under deformation in the relatively short times of exposure used here.

## 4. DISCUSSION

Weight loss determinations and microscopic examinations of specimens tested individually in pyrex capsules showed negligible corrosion ( $\leq 0.1$  mpy) of the candidate materials at 250°C. Weight losses of the mild- and low-alloy steels did continue to increase between 2 weeks and 2 months (but not thereafter), whereas losses of the other materials were essentially the same after 2 weeks, 2 months, and 6 months. When tested in combination with other specimens in stainless steel autoclaves, weight losses of the mild- and low-alloy steels at 250°C were significantly higher than when tested individually. Corrosion rates for these steels over a

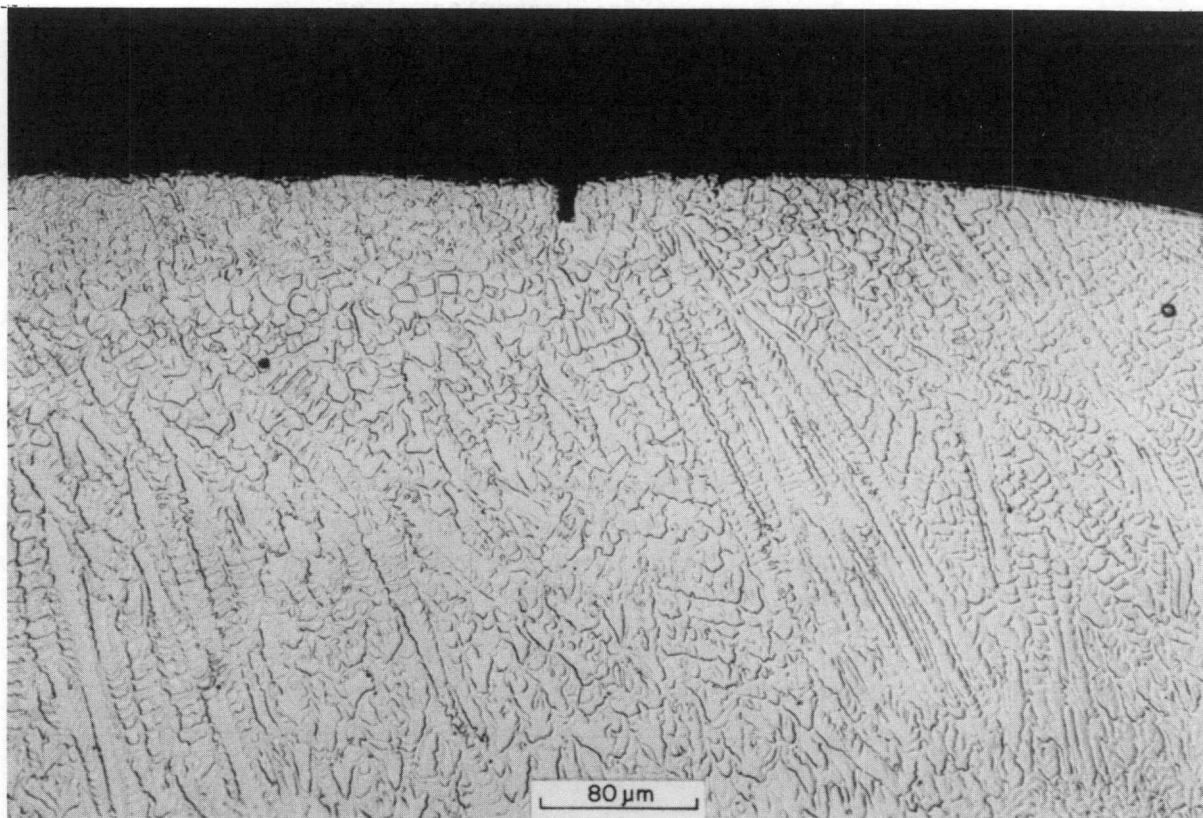


**Fig. 14.** Photomicrograph illustrating the formation of a narrow pit in the weld metal of a Monel 400 specimen after 2 months' exposure to nitrate salts at 250°C.

2-week period in autoclave tests ranged between 0.4 and 1.6 mpy. Two possible causes for the higher rates when these steels were exposed in combination with others are (1) a larger volume of the salt solution compared to the surface area of the susceptible specimens and (2) solubility product effects arising from the presence of dissimilar metals. (All specimens were electrically insulated; therefore, galvanic coupling is not considered a likely cause.) Type 304 stainless steel specimens showed no essential difference in weight loss whether tested individually in pyrex capsules or in the stainless steel autoclave at 250°C. In autoclave tests at lower temperatures (180 and 210°C), weight losses of mild- and low-alloy steels were roughly a factor of 10 less than at 250°C, whereas weight losses of

Table 6. Chemical analyses of solutions removed from capsules after the completion of testing at 250°C

(All entries as concentration, ppm)

Material	Fe	Cr	Ni	Mo	Si
<b>Two-week test period</b>					
Al06B	<2.5	0.12	ND <sup>a</sup>	<0.04	17
Al06B	<2.5	0.12	ND	0.34	19
Cr-Mo	<2.5	0.13	ND	0.04	18
Cr-Mo	<2.5	0.03	ND	0.05	14
<b>Two-month test period</b>					
Al06B	<1.0	<0.3	<0.3	<2.0	<10
Al06B	<1.0	<0.3	<0.3	<2.0	<10
Cr-Mo	<1.0	<0.3	<3.0	<2.0	<10
304	<1.0	<0.3	<0.3	<2.0	<10
304L	<1.0	<0.3	<0.3	<2.0	<10
Monel	<1.0	<0.3	<0.3	<2.0	<10

<sup>a</sup>Not determined.

Table 7. Data summary for constant-strain-rate tests run in nitrate salts at 250°C

Material type	Specimen	Total strain (%)	Average strain rate (min <sup>-1</sup> )	Duration (h)
Al06B	AB-4	8.05	$6.7 \times 10^{-5}$	20
Al06B	AB-5	6.15	$1.6 \times 10^{-5}$	65.5
304L	1-SS	ND <sup>a</sup>	$6.7 \times 10^{-5b}$	20
304L	3-SS	6.00	$1.67 \times 10^{-5}$	66

<sup>a</sup>Not determined.

<sup>b</sup>Estimated from specimen AB-4 run under identical conditions.

type 304 stainless steel were of the same order as at 250°C. The nickel-copper alloy Monel 400 exhibited even lower weight losses than the type 304 stainless steel specimen after 6 months exposure at 250°C, although the actual metal loss of the Monel was offset slightly by the presence of a thin oxide film.

Except for the mild- and low-alloy steels, the corrosion rates recorded in these tests are too low to sort out temperature effects from uncertainties in the measured weight losses. Although both mild- and low-alloy steels showed a significant increase in weight loss after 2 weeks in stainless steel autoclave tests at 250°C compared with 170 and 210°C, tests of these materials in pyrex capsules at 250°C resulted in negligible weight losses even after 6 months. Accordingly, from the standpoint of uniform wall reduction, the present test results would not rule out consideration of any of the reference materials (in mono-metallic systems) for applications even at 250°C. This conclusion is also supported by the appearance of the salt solutions following the tests. In no case did the solutions exhibit a visible change in color; furthermore, the concentrations of metal cations in the solutions remained low, and there was certainly no visual evidence of NO<sub>2</sub> evolution during testing. However, a few widely scattered pits were seen in the case of 2.25Cr-1Mo steel that would require further investigation prior to approving this material for longer-term service.

Very thin oxide films, evidenced by surface darkening, were produced on surfaces of the mild- and low-alloy steels as well as Monel 400. In contrast, surfaces of the type 304 stainless steel remained relatively bright. Although the thickness of these films was extremely superficial even after 6 months, the kinetics of film growth and effects on heat transfer, nevertheless, will require consideration in assessing thermal performance of the lower-alloy steels for long-term service.

A primary purpose of these tests was to gain an assessment of the SCC susceptibility of the selected materials, particularly the mild steels and austenitic stainless steels. When loaded to the elastic limit, there was no evidence of cracking of any of the test materials after 6 months at 250°C. Likewise, there was no evidence of surface cracking or pitting in type 304 stainless steel or Al6B specimens when slowly strained beyond the

elastic limit for 20 and 65 h at 250°C. These results are extremely encouraging with respect to the use of these materials in the higher-temperature ranges required for heat pump applications. However, the conditions leading to SCC are usually quite specific in terms of time, temperature, and electrochemical parameters, and more testing will be required, particularly at temperatures below 250°C and with induced potentials on the test specimens. In the case of mild steels, it will also be important to examine the effect of heat treatment, especially those associated with welding. This was borne out by the severe cracking encountered in the case of steel specimens that did not exhibit the typical pearlite/ferrite microstructure characteristic of A106B.

## 5. CONCLUSIONS

As a result of testing candidate materials for high-temperature CHP applications in nitrate salt solutions at 170 to 250°C, the following conclusions are drawn.

1. When tested as a group in stainless steel autoclaves or individually in pyrex capsules, all of the candidate materials were relatively resistant to concentrated nitrate solutions based on general weight losses and localized corrosion effects. The highest corrosion rates were exhibited by mild steel (A106B) and 2.25Cr-1Mo steel in 2-week tests at 250°C, and these were below 2 mpy. However, these same materials, when tested individually for 6 months in pyrex capsules at 250°C, showed weight losses that translated to a rate of only <0.2 mpy. Therefore, none of the materials included in this test series appears unacceptable from a corrosion standpoint, although more definitive corrosion tests will be required to determine quantitative corrosion rates.

2. With the exception of a "nonstandard" A106B heat, none of the candidate materials exhibited a susceptibility to SCC after a 2-week exposure under constant stress at 170 and 210°C, or after a 6-month exposure at 250°C. Exposures under constant strain rate to strains of 6 and 8% likewise produced no evidence of cracking in type 304 stainless steel and "standard" A106B specimens after 65- and 20-h exposures, respectively, at 250°C.

3. The present tests are useful indicators of the general corrosion resistance of candidate materials; however, they are not intended to provide an absolute measure of corrosion performance under actual heat pump service conditions. The latter objective will require a test program to evaluate (1) corrosion effects accruing from concentration changes associated with evaporation and condensation; (2) electrochemical effects associated with the use of dissimilar metals; (3) effects of extrinsic and intrinsic electric potentials; (4) stress corrosion effects that may occur over the full-service lifetime periods, including "off-normal" conditions; and (5) effects of corrosion product films on heat-transfer performance.

4. Of the materials examined, the mild steel and type 304 stainless steel would appear to offer the best cost/performance indices for industrial heat pumps incorporating nitrate salt solutions. The cracking susceptibility of mild steels, associated with particular microstructural morphologies, will require that a stringent materials quality assurance program be implemented for this class of material.

5. A further caveat in the use of mild steel is that it does form a very tenacious corrosion-product film, and the kinetics of film growth and effects on heat transfer need to be evaluated.

6. The type 304L stainless steel is recommended over type 304 on the basis of its time-proven superior corrosion resistance in the welded state.

## 6. REFERENCES

1. *COR•SUR, Vol. I, Corrosion Data Survey, Metals Section* (computer program), 6th ed., National Association of Corrosion Engineers, Houston, Texas, 1986.
2. W. F. Bogaerts, M. J. Embrechts, and R. Waeben, *Application of the Aqueous Self-Cooled Blanket Concept to a Tritium Producing Shielding Blanket for NET*, EUR-FU/XII-80/87/75, Commission of the European Communities, Brussels, October 1987.



APPENDIX A

WEIGHT CHANGE/DIMENSIONAL DATA AND WELD/STRESS STATUS FOR C-RING  
SPECIMENS USED FOR AUTOCLAVE AND CAPSULE TESTS

Specimen No.	Specimen material	Welded	Stressed	ID (cm)	OD (cm)	Length (cm)	Surface area (cm <sup>2</sup> )	Weight in (g)	Weight out (g)	Exposure (h)
CP001	ASTM-A106	No	Yes	0.9538	1.2611	1.2725	8.0070	3.6781	3.6714	336
CP002	ASTM-A106	No	No	0.9576	1.2637	1.2751	8.0349	3.7049	3.7020	336
CP006	ASTM-A106	Yes	Yes	0.9525	1.2586	1.2560	7.8847	3.5448	3.5416	336
CP007	ASTM-A106	Yes	No	0.9500	1.2611	1.2624	7.9546	3.5462	3.5459	336
CP010	2.25Cr-1Mo	No	Yes	0.9525	1.2649	1.2789	8.0832	3.6266	3.6135	336
CP011	2.25Cr-1Mo	No	No	0.9589	1.2598	1.2611	7.9087	3.5595	3.5556	336
CP015	2.25Cr-1Mo	Yes	Yes	0.9487	1.2637	1.2789	8.0836	3.6209	3.6118	336
CP016	2.25Cr-1Mo	Yes	No	0.9525	1.2662	1.2776	8.0842	3.6112	3.6083	336
CP019	304 SS	Yes	Yes	0.9550	1.2560	1.2700	7.9347	3.6287	3.6286	336
CP020	304 SS	Yes	No	0.9538	1.2573	1.2649	7.9077	3.5986	3.5983	336
CP023	304 SS	No	Yes	0.9589	1.2586	1.2662	7.9311	3.6541	3.6538	336
CP024	304 SS	No	No	0.9576	1.2675	1.2675	8.0413	3.6530	3.6525	336
CP028	304L SS	No	Yes	0.9589	1.2637	1.2713	8.0162	3.6791	3.6788	336
CP029	304L SS	No	No	0.9550	1.2598	1.2624	7.9220	3.6563	3.6553	336
CP034	304L SS	Yes	Yes	0.9500	1.2560	1.2637	7.8890	3.6118	3.6116	336
CP035	304L SS	Yes	No	0.9436	1.2560	1.2662	7.9239	3.5904	3.5904	336
CP037	ASTM-A106	No	Yes	0.9639	1.2624	1.2649	7.9484	3.5810	3.5802	336
CP038	ASTM-A106	No	Yes	0.9639	1.2598	1.2637	7.9156	3.5814	3.5808	336
CP039	ASTM-A106	No	No	0.9614	1.2611	1.2637	7.9344	3.6562	3.6561	336
CP042	ASTM-A106	Yes	Yes	0.9614	1.2560	1.2662	7.8998	3.5364	3.5358	336
CP043	ASTM-A106	Yes	Yes	0.9601	1.2637	1.2611	7.9470	3.5512	3.5502	336
CP044	ASTM-A106	Yes	No	0.9589	1.2573	1.2637	7.9030	3.5898	3.5896	336
CP045	ASTM-A106	Yes	Yes	0.9627	1.2573	1.2662	7.9092	3.5452	3.5445	336
CP047	2.25Cr-1Mo	No	Yes	0.9601	1.2624	1.2611	7.9306	3.5507	3.5502	336
CP048	2.25Cr-1Mo	No	Yes	0.9601	1.2624	1.2662	7.9656	3.5659	3.5650	336
CP049	2.25Cr-1Mo	No	No	0.9627	1.2611	1.2649	7.8797	3.5284	3.5281	336
CP050	2.25Cr-1Mo	No	Yes	0.9627	1.2637	1.2637	7.9563	3.5608	3.5591	336
CP052	2.25Cr-1Mo	Yes	Yes	0.9665	1.2675	1.2624	7.9767	3.6225	3.6218	336
CP053	2.25Cr-1Mo	Yes	Yes	0.9665	1.2649	1.2573	7.9165	3.5954	3.5948	336
CP054	2.25Cr-1Mo	Yes	No	0.9652	1.2649	1.2598	7.9430	3.5970	3.5966	4752
CP055	2.25Cr-1Mo	Yes	No	0.9665	1.2649	1.2637	7.9555	3.6152	3.6151	336
CP056	304 SS	No	No	0.9639	1.2649	1.2637	7.9657	3.8994	3.8990	336
CP057	304 SS	No	Yes	0.9614	1.2649	1.2637	7.9720	3.9212	3.9206	336
CP058	304 SS	No	Yes	0.9601	1.2675	1.2624	7.9809	3.9293	3.9287	336
CP059	304 SS	No	Yes	0.9614	1.2662	1.2598	7.9612	3.9137	3.9129	336
CP061	304 SS	Yes	No	0.9665	1.2662	1.2586	7.9446	3.8844	3.8839	336
CP062	304 SS	Yes	Yes	0.9639	1.2649	1.2611	7.9501	3.9060	3.9055	336

APPENDIX A (Continued)

Specimen No.	Specimen material	Welded	Stressed	ID (cm)	OD (cm)	Length (cm)	Surface area (cm <sup>2</sup> )	Weight in (g)	Weight out (g)	Exposure (h)
CP063	304 SS	Yes	Yes	0.9627	1.2649	1.2611	7.9571	3.9165	3.9162	336
CP064	304 SS	Yes	No	0.9652	1.2662	1.2598	7.9517	3.8768	3.8765	4752
CP065	304 SS	Yes	Yes	0.9665	1.2649	1.2637	7.9594	3.8939	3.8936	1440
CP066	304 SS	Yes	Yes	0.9665	1.2662	1.2611	7.9564	3.9108	3.9103	336
CP067	Monel	No	No	0.9614	1.2560	1.2662	7.8998	3.9192	3.9189	336
CP068	Monel	No	Yes	0.9614	1.2560	1.2611	7.8610	3.9699	3.9695	336
CP069	Monel	No	Yes	0.9589	1.2586	1.2637	7.9078	4.0446	4.0443	336
CP070	Monel	No	Yes	0.9614	1.2560	1.2611	7.8571	4.0009	3.9993	336
CP072	Monel	Yes	No	0.9601	1.2560	1.2637	7.8718	4.0307	4.0307	336
CP073	Monel	Yes	Yes	0.9614	1.2573	1.2662	7.9006	4.0191	4.0184	336
CP074	Monel	Yes	Yes	0.9614	1.2586	1.2662	7.9209	4.0117	4.0117	336
CP075	Monel	Yes	No	0.9601	1.2560	1.2662	7.8990	4.0259	4.0265	4752
CP076	Monel	Yes	Yes	0.9639	1.2560	1.2637	7.8780	4.0173	4.0170	1440
CP077	304L SS	No	No	0.9627	1.2637	1.2611	7.9407	3.5655	3.5653	336
CP078	304L SS	No	Yes	0.9614	1.2637	1.2611	7.9361	3.6482	3.6480	336
CP079	304L SS	No	Yes	0.9614	1.2662	1.2611	7.9689	3.6588	3.6587	336
CP080	304L SS	No	Yes	0.9601	1.2662	1.2611	7.9721	3.6713	3.6709	336
CP082	304L SS	Yes	No	0.9665	1.2687	1.2624	7.9893	3.6763	3.6763	336
CP083	304L SS	Yes	Yes	0.9614	1.2611	1.2560	7.8761	3.6075	3.6073	336
CP084	304L SS	Yes	Yes	0.9627	1.2649	1.2624	7.9572	3.6472	3.6470	336
CP085	304L SS	Yes	No	0.9639	1.2649	1.2637	7.9657	3.6392	3.6393	4752
CP086	ASTM-A106	No	Yes	0.9627	1.2510	1.2637	7.8311	3.4146	3.4153	4752
CP087	ASTM-A106	No	No	0.9639	1.2586	1.2624	7.8953	3.4082	3.4084	336
CP088	ASTM-A106	No	Yes	0.9627	1.2535	1.2637	7.8404	3.4268	3.4267	336
CP089	ASTM-A106	No	Yes	0.9627	1.2535	1.2624	7.8366	3.4355	3.4354	336
CP090	ASTM-A106	No	Yes	0.9639	1.2560	1.2637	7.8662	3.4564	3.4560	1440
CP091	ASTM-A106	Yes	No	0.9614	1.2471	1.2611	7.7695	3.3417	3.4170	4752
CP092	ASTM-A106	Yes	No	0.9589	1.2446	1.2637	7.7702	3.3434	3.3437	336
CP093	ASTM-A106	Yes	Yes	0.9601	1.2395	1.2611	7.7018	3.2780	3.2779	336
CP094	ASTM-A106	Yes	Yes	0.9589	1.2484	1.2611	7.7923	3.3984	3.3981	336
CP095	ASTM-A106	Yes	Yes	0.9589	1.2357	1.2624	7.6752	3.3267	3.6261	1440
CP101	2.25Cr-1Mo	Yes	Yes	0.9741	1.2764	1.2713	8.0852	3.6259	3.6242	1440
CP102	2.25Cr-1Mo	Yes	Yes	0.9690	1.2776	1.2687	8.1025	3.6263	3.6245	336
CP109	Monel	Yes	Yes	0.9639	1.2840	1.2738	8.2174	4.2256	4.2246	336
CP113	ASTM-B106	No	Yes	0.9690	1.2700	1.2611	7.9862	3.6631	3.6621	336
CP118	ASTM-B106	Yes	Yes	0.9677	1.2700	1.2687	8.0223	3.6442	3.6433	336
CP136	304L SS	Yes	Yes	0.9665	1.2738	1.2700	8.0672	3.6943	3.6941	1440
CP137	304L SS	Yes	Yes	0.9665	1.2738	1.2700	8.0865	3.7156	3.7155	336

## APPENDIX B

## CHP CAPSULE PREPARATION PROCEDURE

OBJECTIVE: Description of technique for the fabrication of pyrex capsules used in the CHP corrosion tests.

1. The glass shop prepares closed-end cylinders using cleaned 25-mm OD by 1.5-mm wall pyrex tubing stock, finishing to an overall length of approximately 0.3 m (12 in.). Following closure, the tube is annealed.

2. The corrosion group prepares and inserts one or more C-ring specimens into the closed tube.

3. Using normal bench-burner techniques, the glass shop constricts the open end of the pyrex tube at a point about 20 cm (8 in.) above the closed end (specimen position). The constriction is approximately 3.75-cm (1-1/2 in.) long by 4.8 mm (3/16 in.) ID, the wall being upset to a thickness of approximately 3 mm. The specimen is not allowed to be heated during this operation.

4. The corrosion group prepares and injects 20 mL of the corrodant through the constriction in the tube, totally immersing the C-ring specimen. Care is taken to avoid contact of the corrodant solution with the constricted region.

5. The glass shop attaches the upper (unconstricted) end of the capsule to a roughing pump and evacuates it, taking care to throttle the air flow so as to avoid violent bubbling of the liquid during decompression. After approximately 5 min of evacuation, the glassblower preheats the constriction lightly and then proceeds to flame seal the capsule.

6. In the sealing operation, the glass blower utilizes flame size and application to form a desirable final geometry inside the end of the sealed constriction. This operation is critical, as improper seal-off operations result in undesirable seal geometries which, in turn, lead to capsule failure during testing. Finally, the sealed constriction is gently annealed to minimize residual stresses.



## APPENDIX C

## CONSTANT-STRAIN-RATE TEST PROCEDURE

## Start-Up

1. Remove top of autoclave with pull-rod assembly from autoclave and install specimen.
2. Reinstall assembly in the autoclave containing specified nitrate mix at 50°C.
3. Evacuate autoclave for 5 min, then valve out vacuum pump.
4. Increase autoclave temperature to desired operating level.
5. Mechanically adjust pull rod and load-train coupling until a positive load is indicated on the load-cell recorder.
6. Record dial indicator reading.
7. Adjust gear ratio and motor speed of reduction gear drive to settings corresponding to desired strain rate.
8. Switch on reduction gear drive and monitor dial indicator to verify the desired strain rate.
9. Record the following start-up information.
10. Test starting time and date, test ending time and date, chart scale and speed, cross head speed, and initial and final dial indicator reading.

## Shutdown

1. Turn off reduction gear drive and power input.
2. Initiate load release at termination of planned test time.
3. Monitor autoclave cooling, removing load as required to avoid stressing specimen through contraction of pull-rod assembly on cooling.



## INTERNAL DISTRIBUTION

- |                                    |                                   |
|------------------------------------|-----------------------------------|
| 1-2. Central Research Library      | 22. W. Fulkerson                  |
| 3. Document Reference Section      | 23. R. R. Judkins                 |
| 4-5. Laboratory Records Department | 24. J. R. Keiser                  |
| 6. Laboratory Records, ORNL RC     | 25. A. C. Schaffhauser            |
| 7. ORNL Patent Section             | 26. G. M. Slaughter               |
| 8-10. M & C Records Office         | 27. P. F. Tortorelli              |
| 11. M. R. Ally                     | 28. D. F. Wilson                  |
| 12. W. D. Bond                     | 29. A. D. Brailsford (Consultant) |
| 13. R. A. Bradley                  | 30. H. D. Brody (Consultant)      |
| 14. R. S. Carlsmith                | 31. F. F. Lange (Consultant)      |
| 15. D. F. Craig                    | 32. D. Pope (Consultant)          |
| 16-20. J. H. DeVan                 | 33. E. R. Thompson (Consultant)   |
| 21. J. R. DiStefano                | 34. J. B. Wachtman (Consultant)   |

## EXTERNAL DISTRIBUTION

- |  |  |
|--|--|
| 35. Dr. V. Aronov<br>IIT Research Institute<br>10 W. 35th Street<br>Chicago, IL 60616            | 41. Dr. R. Dwivedi<br>IIT Research Institute<br>10 W. 35th Street<br>Chicago, IL 60616   |
| 36. Dr. Joseph Au<br>Sunstrand Aviation<br>P.O. Box 7102<br>Rockford, IL 61125                   | 42. Dr. Ratnesh Dwivedi<br>Lanxide Corporation<br>Tralee Industrial Park<br>Newark, DE 19711                                     |
| 37. Mr. Deane I. Biehler<br>Caterpillar Tractor Co.<br>100 N. E. Adams<br>Peoria, IL 61629       | 43. Dr. J. J. Eberhardt<br>Department of Energy<br>ECUT Division, CE-12<br>1000 Independence Ave., S. W.<br>Washington, DC 20585 |
| 38. Mr. John Boppart<br>Garrett Turbine Engine Company<br>P.O. Box 5217<br>Phoenix, AZ 85010     | 44. Mr. Jim Edler<br>Eaton Corp.<br>26201 Northwestern Highway<br>P.O. Box 766<br>Southfield, MI 48037                           |
| 39. Mr. Gary M. Crosbie<br>Ford Motor Company<br>Dearborn, MI 48121                              | 45. Dr. Ali Erdemir<br>Argonne National Laboratory<br>Bldg. 212<br>9700 S. Cass Avenue<br>Argonne, IL 60439                      |
| 40. Mr. Keith Dufrane<br>Battelle Columbus Laboratories<br>505 King Avenue<br>Columbus, OH 43201 |  |

46. Dr. George Fenske  
Argonne National Laboratory  
Bldg. 212  
9700 S. Cass Avenue  
Argonne, IL 60439
47. Mr. Jim Greenleaf  
Greenleaf Corp.  
25019 Viking Street  
Hayward, CA 94545
48. Dr. Nabil Hakim  
General Motors  
Detroit Diesel Allison  
Romulus, MI 48174
49. Dr. Stephen Hsu  
National Institute of Standards  
and Technology  
Ceramics Division  
Gaithersburg, MD 20899
50. Dr. Said Jahanmir  
National Institute of Standards  
and Technology  
Met. A 215  
Gaithersburg, MD 20899
51. Dr. Joe Lane  
National Matls Advisory Board  
2101 Constitution Avenue  
Washington, DC 20418
52. Dr. Jorn Larsen-Basse  
National Science Foundation  
1800 G. St., N.W. (Rm 1110)  
Washington, DC 20550
53. Dr. David Lewis  
Naval Research Lab  
Washington, DC 20375
54. Mr. John Lucek  
Norton Company  
Goddard Road  
Northborough, MA 01532
55. Dr. John McCool  
250 Ridge Pike, Apt. 150B  
Lafayette Hill, PA 19444
56. Dr. P. K. Mehrotra  
Kennemetal  
P.O. Box 639  
Greensburg, PA 15601
- 57-59. Mr. David G. Mello  
Department of Energy  
ECUT Division, CE-12  
1000 Independence Ave., S. W.  
Washington, DC 20585
60. Dr. Allan I. Michaels  
Argonne National Laboratory  
Bldg. 212  
9700 S. Cass Avenue  
Argonne, IL 60439
61. Mr. John Morrow  
FMC Corporation  
1105 Coleman Avenue, Box 1201  
San Jose, CA 95108
62. Dr. Malcolm Naylor  
Cummins Engine Co.  
Box 3005  
Columbus, IN 45202-3005
- 63-72. Dr. Fred A. Nichols  
Argonne National Laboratory  
Bldg. 212  
9700 S. Cass Avenue  
Argonne, IL 60439
73. Mr. E. D. Porter  
Ferro Corporation  
661 Willet Road  
Buffalo, NY 14218-9990
74. Dr. A. W. Ruff  
National Institute of Standards  
and Technology  
Met. A 215  
Gaithersburg, MD 20899
75. Dr. William Schumacher  
Armco Steel Corp.  
703 Curtis Street  
Middletown, OH 45043

76. Dr. T. Spalvins  
NASA Lewis Research Center  
MS 23-2  
21000 Brookpark Road  
Cleveland, OH 44135
77. Dr. M. Srinivasan  
Standard Oil Engr'd Matls Co.  
P.O. Box 832  
Niagara Falls, NY 14302
78. Dr. Paul Swanson  
Deere and Company Tech. Center  
3300 River Drive  
Molene, IL 61265
79. B.-Y Ting  
School of Mechanical Engr.  
Georgia Institute of Tech.  
Atlanta, GA 30332-0420
80. Dr. Ed Van Reuth  
Technology Strategies Corp.  
10722 Shingle Oak Court  
Burke, VA 22015
81. Prof. James J. Wert  
Metall. Dept. (Box 1621  
Sta. B)  
Vanderbilt University  
Nashville, TN 37235
82. Dr. A. C. Westwood  
Martin Marietta Laboratories  
1450 S. Rolling Road  
Baltimore, MD 21227
83. Prof. Ward O. Winer  
School of Mechanical Engr.  
Georgia Institute of Tech.  
Atlanta, GA 30332-0420
- 84-88. Dr. James S. Wolf  
Department of Mechanical  
Engineering  
Clemson University  
Clemson, SC 29634-0921
89. DOE, Oak Ridge Operations  
Office  
Office of Assistant Manager  
for Energy Research and  
Development  
P.O. Box 2001  
Oak Ridge, TN 37831-8600
- 90-99. Office of Scientific and  
Technical Information  
Office of Information Services  
P.O. Box 62  
Oak Ridge, TN 37831
- For distribution by microfiche  
as shown in DOE/OSTI-4500,  
Distribution Category UC-95e  
(Energy Conservation-Waste  
Systems and Utilization)

